Effect of Kinetics on Residue Curve Maps for Reactive Distillation

Ganesh Venimadhavan, George Buzad, Michael F. Doherty, and Michael F. Malone
Dept. of Chemical Engineering, University of Massachusetts, Amherst, MA 01003

A class of models is derived for studying the effects of chemical kinetics on residue curve maps for reactive distillation. Activity-based rate and phase equilibrium expressions provide an accurate and thermodynamically consistent description of composition changes in nonideal, reacting vapor-liquid mixtures. For certain strategies of operation, which dictate the rate of product removal, the model equations are nonautonomous, leading to unusual dynamic behavior. However, for a certain special product removal policy, the effects of kinetics can be described by a single parameter, the Damköhler number, which measures the rate of reaction relative to product removal. For small values of the Damköhler number, the nonreactive simple distillation residue curve map is recovered and the singular points are the pure components and azeotropes in the nonreactive mixture. A bifurcation analysis shows the deformation and, in some cases, the disappearance of these singular points as the Damköhler number is increased until the equilibrium reactive residue curve map is recovered at large values. This bifurcation analysis reveals the limitations of the equilibrium analysis. A model problem for the reactive distillation of methyl tert-butyl ether from isobutene and methanol is solved.

Introduction

Distillation accompanied by chemical reaction is a process alternative that has the potential to lower process costs and reduce environmental emissions (Agreda et al., 1984, 1990; Grosser et al., 1987; Smith, 1981, 1990). Reactive distillation is not advantageous in every case, however, and there is a need for systematic methods to decide when it should be used and when it should not. Literature on design and synthesis methods for equilibrium reactive distillation is growing (see the review by Doherty and Buzad, 1992), which needs to be generalized to systems where chemical kinetics plays an important role.

A concept that has found wide utility in recent years is the simple distillation residue curve map. It has been used by numerous authors to aid in the design, synthesis and analysis of nonreactive distillation systems. It has also been used as a tool for understanding distillation with equilibrium chemical reactions (Barbosa and Doherty, 1988). This article presents the effect of chemical kinetics on residue curve maps for reactive simple distillation.

The effect of kinetics on the simple distillation of mixtures accompanied by chemical reaction in the liquid phase has also been studied by Solokhin et al. (1990a,b). They considered the general case of multiple reactions and gave detailed results for the two special cases, $A \Leftrightarrow B$ and $2A \Leftrightarrow B + C$. The differential equations that they developed for these cases were nonautonomous: they had an explicit time-dependence on the righthand side of the equation. We show that their model is just one example of a family of models, which we derive in this article.

We start by looking at a simplified model system, with equimolar stoichiometry. A mathematical model is developed for this system and used to generate residue curves for different values of the characteristic parameters. Following this, the model is developed for a more general stoichiometry and then applied to the reactive mixture of isobutene, methanol and methyl tert-butyl ether (MTBE).

A Simple Example

We consider a liquid-phase reaction with stoichiometry $A + B \Leftrightarrow 2C$. We assume that the liquid is an ideal mixture and that the reaction is elementary. The rate of reaction per mole of mixture is given by

$$r_A = r_B = -\frac{r_C}{2} = -k_f\left(x_1 x_2 - \frac{x_3^2}{K}\right) \tag{1}$$

Components 1, 2 and 3 correspond to A, B, and C, respectively, K is the thermodynamic equilibrium constant, and k_f is the forward reaction rate constant. We use mole fractions in the rate expressions, rather than concentrations, because they conform more naturally to the method of writing material balances and vapor-liquid equilibrium models for distillation problems. This approach also has the advantage of giving a rate constant with units of reciprocal time regardless of the order of the reaction, allowing for a simple universal definition of the dimensionless Damköhler number for all reaction orders. More importantly, as we shall show later, this kinetic form and a more general form based on the activities can give an accurate description of rate *and* equilibrium data.

The overall and component material balances for simple distillation (Figure 1) are

$$\frac{dH}{dt} = -V \tag{2}$$

and

$$\frac{dHx_i}{dt} = -Vy_i - Hk_f\left(x_1x_2 - \frac{x_3^2}{K}\right) \quad (i=1,2) \tag{3}$$

Expanding the derivative in Eq. 3 and incorporating Eq. 2 give

$$H\frac{dx_i}{dt} - Vx_i = -Vy_i - Hk_f\left(x_1x_2 - \frac{x_3^2}{K}\right) \quad (i=1,2) \tag{4}$$

Dividing Eq. 4 by V and rearranging give

$$\frac{dx_i}{d\xi} = x_i - y_i - Da\left(x_1x_2 - \frac{x_3^2}{K}\right)\frac{H}{H_0}\frac{k_f}{k_{f,\min}}\frac{V_0}{V} \quad (i=1,2) \tag{5}$$

where $d\xi = (V/H)dt$. The Damköhler number, $Da = H_0k_{f,\min}/V_0$, is a dimensionless ratio of a characteristic liquid residence time (H_0/V_0) to the characteristic reaction time ($1/k_{f,\min}$). The quantity $k_{f,\min}$ is the value of the forward rate constant at the lowest temperature on the boiling surface (the lowest boiling azeotrope or pure component in the system). The ratio $k_f/k_{f,\min}$ is expected to be a monotonically increasing function of temperature and therefore monotonically increases along the residue curves. For this example, we take k_f to be constant with a value of $k_{f,\min}$. Solving for the ratio H/H_0 by rearranging Eq. 2

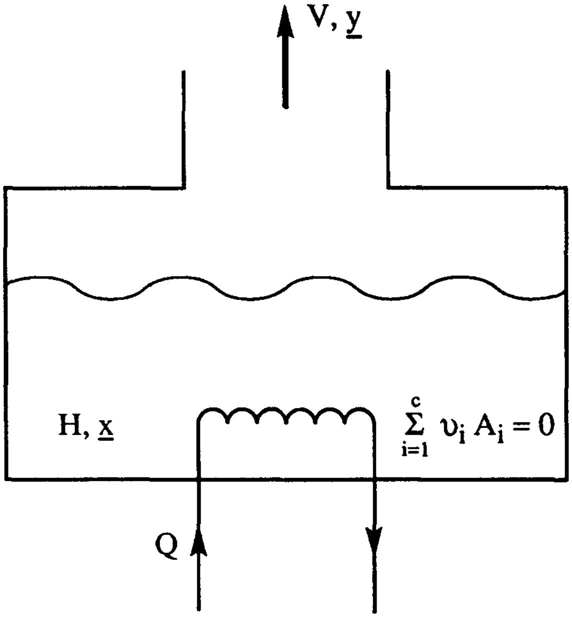

Figure 1. Simple reactive distillation process.

$$\frac{dH}{d\xi} = -H, \quad H(\xi=0) = H_0 \tag{6}$$

and integrating gives the result

$$\frac{H}{H_0} = e^{-\xi} \tag{7}$$

Equation 5 can be written as

$$\frac{dx_i}{d\xi} = x_i - y_i - Da\left(x_1x_2 - \frac{x_3^2}{K}\right)\frac{V_0}{V}e^{-\xi} \quad (i=1,2) \tag{8}$$

This is the basic equation that must be solved to obtain the residue curves for simple distillation. In contrast to results for the equilibrium theory (Barbosa and Doherty, 1988; Ung and Doherty, 1994b), Eq. 8 cannot be solved without first specifying a policy for V/V_0 (and thus implicitly a heating policy). Here, "policy" refers to the adjustment made, such as to the heating rate, to control the rate at which vapor is removed from the still. One possibility is to use a heating policy that will give V/V_0 equal to H/H_0, which gives

$$\frac{dx_i}{d\xi} = x_i - y_i - Da\left(x_1x_2 - \frac{x_3^2}{K}\right) \quad (i=1,2) \tag{9}$$

Another alternative is to use a heating policy that keeps $V = V_0$ for all times. This situation is close to what happens with a constant rate of heating policy (it is exact when all the components have the same heats of vaporization and when there is no heat of mixing or reaction). With such a policy Eq. 8 becomes

$$\frac{dx_i}{d\xi} = x_i - y_i - Da\left(x_1x_2 - \frac{x_3^2}{K}\right)e^{-\xi} \quad (i=1,2) \tag{10}$$

Both of these models and many others represent the simple distillation process subject to a particular heating policy. In the first case, Eq. 9, the model is autonomous whereas in the second case (Eq. 10) the model is nonautonomous. Nonautonomous differential equations are not common in chemical engineering applications, but their qualitative properties are described in the mathematical literature. Nonautonomous systems have certain properties which make their study both interesting and difficult. These include the fact that, unlike the autonomous case, the forward and reverse problems are not equivalent in the nonautonomous problem $[\underline{f}(\underline{x},t) \neq \underline{f}(\underline{x},-t)]$. Another interesting property of nonautonomous equations is that the initial condition cannot be shifted in time $[\underline{f}(\underline{x}_0,t_0) \neq \underline{f}(\underline{x}_0,t_0+s),\ s \neq 0]$. A direct consequence of this is that, while the integral curves are unique, the trajectories are not: trajectories may intersect themselves and each other in the phase plane (Davies and James, 1966; Sansone and Conti, 1964). We solve for simple distillation residue curve maps using both the autonomous case (Eq. 9) and the nonautonomous case (Eq. 10).

Calculation of Residue Curve Maps

Consider the simple distillation of a ternary mixture that undergoes a reversible reaction

$$A+B \Leftrightarrow 2C \tag{11}$$

with an equilibrium constant $K=2$, which is assumed to be independent of temperature. We will also assume that the three components form an ideal mixture whose vapor liquid equilibrium behavior can be described using constant volatilities of components A and B relative to C of 5 and 3, respectively. In all cases, the kinetic residue curve maps were generated by taking initial conditions around the periphery of the composition triangle. For reference, the simple distillation residue curve map for the nonreactive mixture is shown in Figure 2. Barbosa and Doherty (1988) studied the case when the reaction reaches equilibrium instantaneously and showed that a reactive azeotrope may appear. In fact, for the parameter values selected, a maximum boiling reactive azeotrope does occur, as shown in Figure 3.

Let us now see how the presence of a finite rate of reaction influences the simple distillation process. First, consider the autonomous model (Eq. 9) for a mixture with a large value for *Da*, that is, a very fast forward reaction. Figure 3 shows the residue curve map at $Da=100$; at high values of *Da*, this model recovers the chemical equilibrium limit at long times.

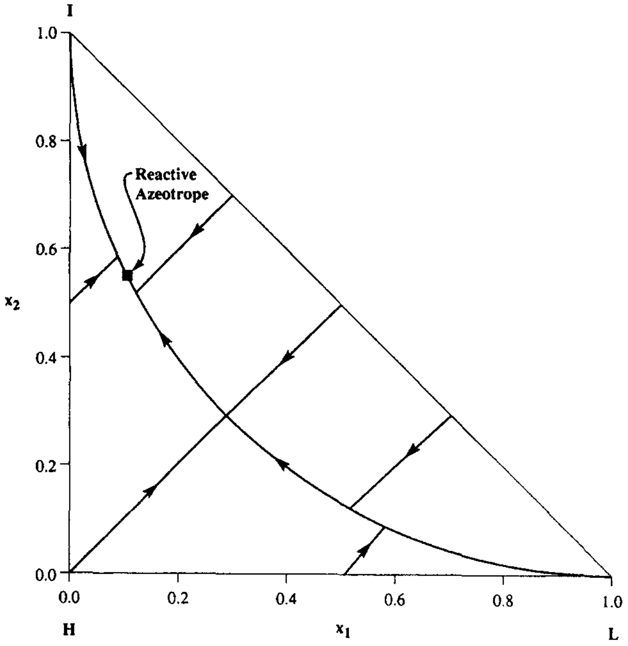

Figure 3. Residue curve map at $Da=100$ for a reactive mixture with the reaction $A+B \Leftrightarrow 2C$ for which the volatilities of components A and B relative to C are 5 and 3, respectively.

The reaction equilibrium constant is equal to 2.

The nonautonomous model (Eq. 10), on the other hand, gives the residue curve map shown in Figure 4 at $Da=100$. As time increases, the residue curves do not approach the reactive azeotrope, but approach the heaviest component instead. This can be explained from the form of the model equations, where the

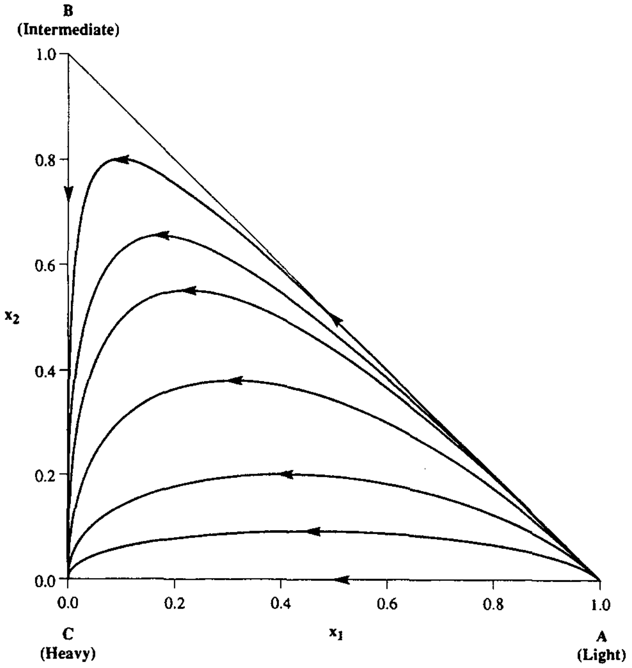

Figure 2. Residue curve map for a nonreactive mixture for which volatilities of components A and B relative to C are 5 and 3, respectively.

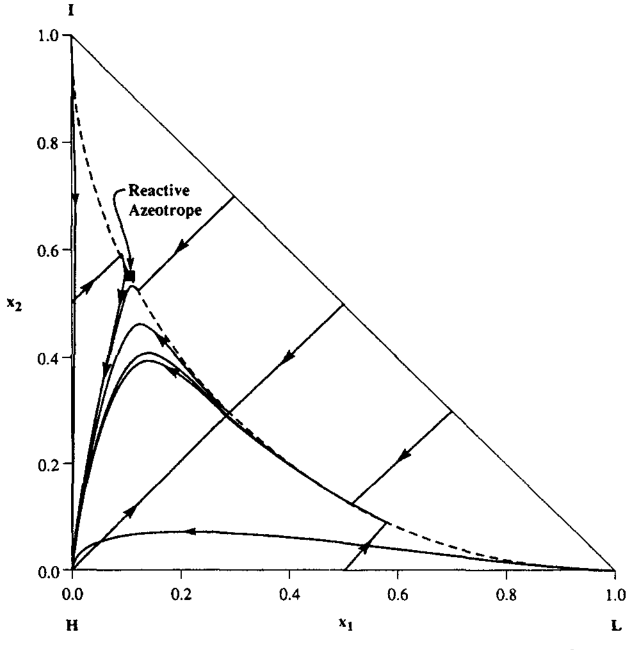

Figure 4. Residue curve map at $Da=100$ for the mixture in Figure 3 using Eq. 10.

Dashed line shows the position of the reaction equilibrium curve.

warped time appears explicitly in the reaction term as $e^{-\xi}$. Initially this exponential term is on the order of unity so the presence of the reaction is felt, especially at large values of *Da* (Figure 4); for example, the residue curves initially move toward the equilibrium curve. At large values of ξ, however, the exponential term is small and Eq. 10 approaches the nonreactive limit. Thus, it is not surprising that the residue curves approach the heaviest component at long times.

We now show a selection of residue curve maps at other values of *Da*. First, we will consider the nonautonomous model. Figure 5 shows the residue curve maps at values of *Da* equal to 5 and 1, respectively. At large times, the residue curves behave essentially as they did at $Da = 100$, namely, they approach the heaviest component. At short times, however, they differ in that the residue curves do not approach the reaction equilibrium curve closely at small values of *Da* (Figure 5b) as they do at larger values of *Da*. Figures 6a and 6b show residue curve maps for the autonomous model at values of *Da* equal to 5 and 1, respectively. Note that the residue curves are no longer constrained by the reaction equilibrium curve and that the residue curves terminate at different locations (approach

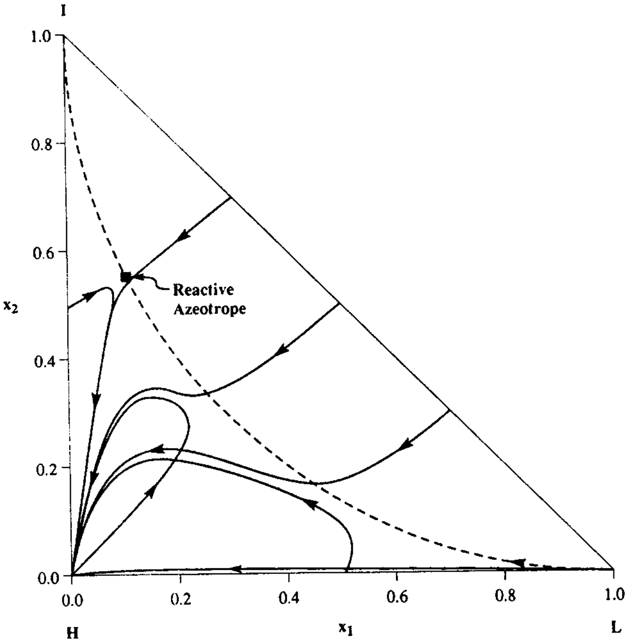

Figure 5(a). Residue curve map at $Da = 5$ for the mixture in Figure 3 using Eq. 10.

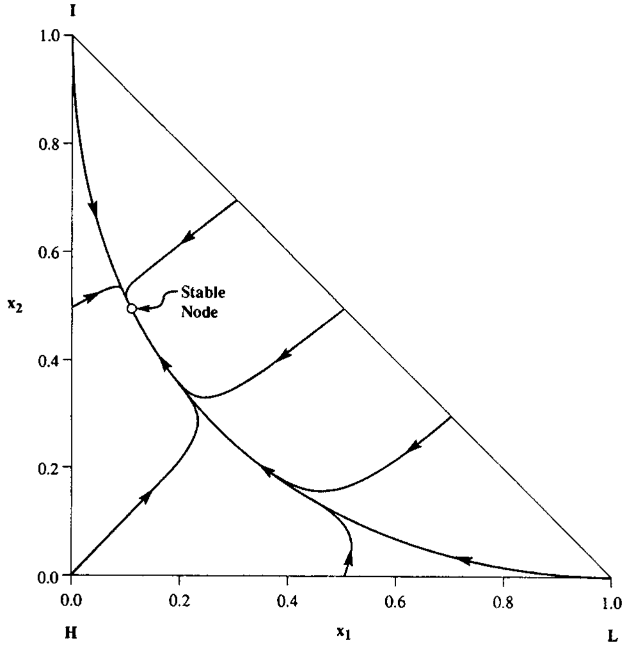

Figure 6(a). Residue curve map at $Da = 5$ for the mixture in Figure 3 using Eq. 9.

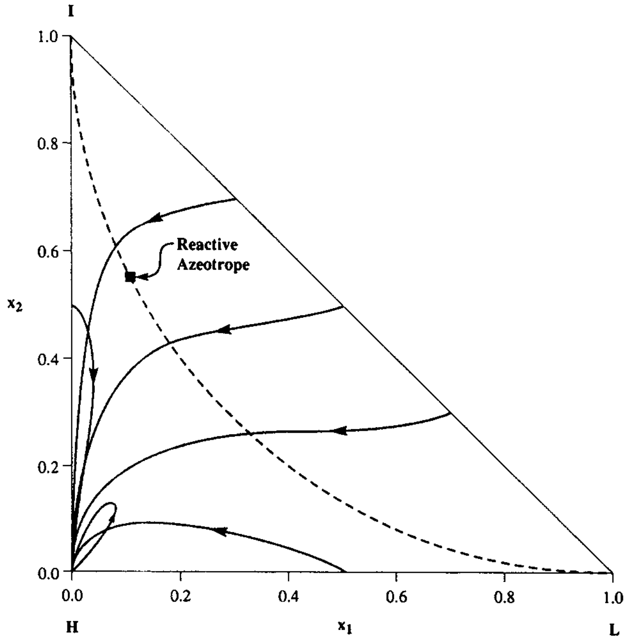

Figure 5(b). Residue curve map at $Da = 1$ for the mixture in Figure 3 using Eq. 10.

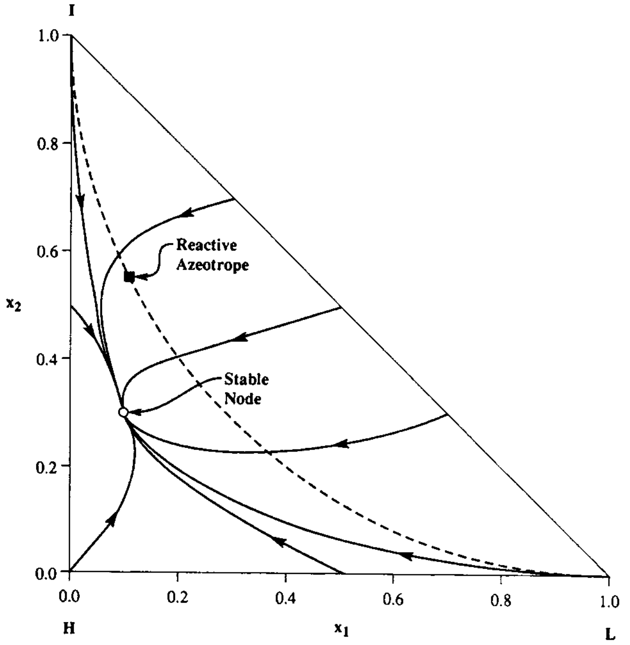

Figure 6(b). Residue curve map at $Da = 1$ for the mixture in Figure 3 using Eq. 9.

a stable node at a different composition) as the value of *Da* is changed. We can solve for this stable node from Eq. 9.

$$0 = x_i - y_i - Da\left(x_1 x_2 - \frac{x_3^2}{K}\right) \quad (i = 1,2) \qquad (12)$$

Equations 12 have multiple solutions. It is easy to show that the pure component *B* vertex ($x_1 = x_3 = 0$) and the pure component *A* vertex ($x_2 = x_3 = 0$) are solutions, but pure component *C* is not. (See Appendix for an asymptotic analysis of Eq. 9.) These "trivial," pure component solutions are independent of the value of the Damköhler number and the thermodynamic equilibrium constant. We are more interested in nontrivial feasible solutions, which are affected by the variation in the values of *Da* and *K*. Figure 7 shows the single nontrivial singular point for the mixture under consideration at several values of *Da*. The singular point originates at the maximum boiling reactive azeotrope at large values of *Da* and moves toward the heaviest component as *Da* decreases, until in the limit of *Da* equal to zero the singular point corresponds to the composition of the heaviest component (component *C*). The curve in Figure 7 represents a branch of stable nodes parameterized by *Da*.

There are two characteristic parameters for this model: the Damköhler number, *Da*, and the thermodynamic equilibrium constant, *K*. A large value of *Da*, for a given ratio of H_0/V_0, implies a very fast forward reaction, while a small *Da* implies a slow forward reaction. A large value of *K* means that the forward reaction rate constant is much larger than the reverse reaction rate constant, and the equilibrium curve is closer to the pure *C* vertex of the triangle (see Figure 8). This implies that the reaction is nearly irreversible. A small value of *K* means that the forward reaction is very slow and the reverse reaction is very fast. This implies that the equilibrium curve is close to the *A-B* edge, as shown in Figure 8. See Table 1 for a summary of the interplay between *Da* and *K*.

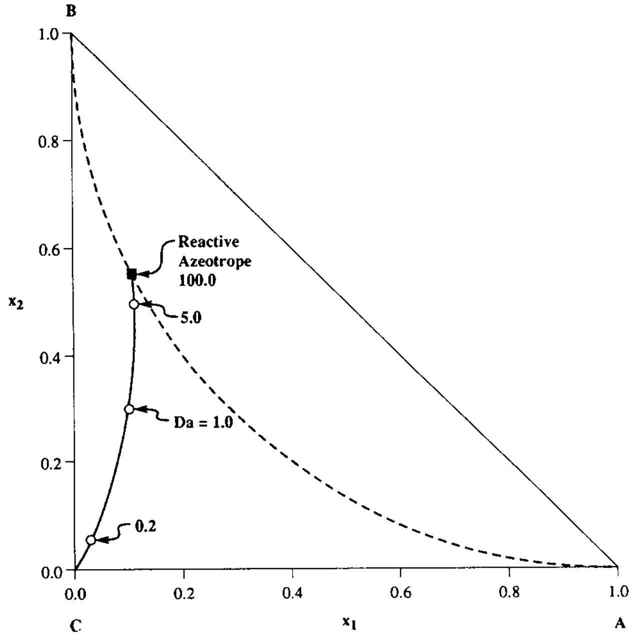

Figure 7. Singular points of Eq. 9 for the mixture in Figure 3 at several values of *Da*.

Dashed line represents the reaction equilibrium curve.

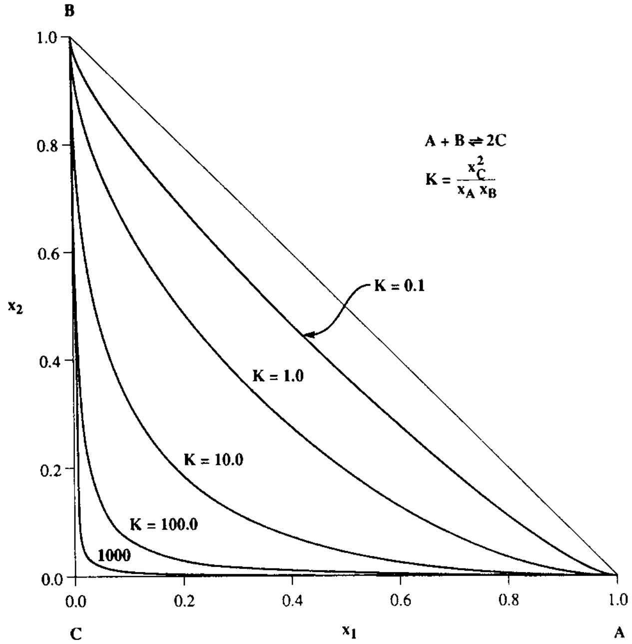

Figure 8. Position of the equilibrium curve as a function of *K* for the reaction $A + B \Leftrightarrow 2C$ when the components form an ideal liquid mixture.

Parametric Sensitivity

In the above example, we considered a constant vapor rate policy, which led to the nonautonomous model and a policy in which the vapor rate changes in exactly the same manner as the liquid holdup in the still. For the first policy, the lighter components are driven off at a rapid rate and all the trajectories finally approach the pure *C* vertex (Figures 4 and 5). In the second policy, the trajectories approach a common curve and terminate at a stable node. For large values of *Da*, the common curve is the equilibrium curve, and the stable node corresponds to the reactive azeotrope. We have seen that the position of the stable node changes by changing the Damköhler number and the thermodynamic equilibrium constant. While this is an

Table 1. Summary of the Interplay between *Da* and *K*

Da	*K*	Remarks
Low	Low	Slow forward reaction; fast backward reaction; little or no product formation
Low	High	Slow forward reaction; slower reverse reaction; high product formation
High	Low	Fast forward reaction; faster backward reaction; little product formation; equilibrium curve near the *A-B* edge
High	High	Fast forward reaction; slow backward reaction; essentially an irreversible instantaneous reaction

interesting case, the vapor rate policy that brings it about is rather restrictive, and it is of interest to study the effect of different vapor rate policies on the still paths.

We assume $V=V_0e^{\epsilon\xi}$, and Eq. 8 becomes

$$\frac{dx_i}{d\xi}=x_i-y_i-Da\left(x_1x_2-\frac{x_3^2}{K}\right)e^{-(1+\epsilon)\xi} \tag{13}$$

The two policies discussed earlier are just specific examples of this form, with $\epsilon=-1$ in the first case (the decreasing vapor rate policy that makes $V/V_0=H/H_0$, and gives Eq. 9), and $\epsilon=0$ in the second (the constant vapor rate policy, $V=V_0$, which gives Eq. 10). We found that for any value of $\epsilon>0$ (which means that the vapor rate increases with time), the trajectories terminate at the pure C vertex (just as in the $\epsilon=0$ case). This is because the vapor rate is large enough so that the reaction cannot "keep up" with the vaporization. For values of $\epsilon<-1$ (this means that the vapor rate decreases faster than the liquid holdup in the still), the trajectories terminate at the stable node, just as in the $\epsilon=-1$ case. For ϵ between 0 and -1, the behavior of the trajectories is between those for $\epsilon\geq 0$ and $\epsilon\leq -1$. The still paths approach the common curve, stay on it for a finite time and then turn toward the pure component C vertex. We can therefore conclude that the results obtained for the policy $V/V_0=H/H_0$ hold qualitatively for other policies ($V/V_0<H/H_0$), and that they are not artifacts of the specific policy.

A more general system

In the previous example, we studied a mixture of just three species. We also ensured that the number of moles in the system was conserved by a specific choice of stoichiometry and we used a very simple description of the equilibrium and kinetic behavior. We now relax the assumptions. We still assume, however, that there is only one reaction in the liquid phase which we can represent by

$$\sum_{m=1}^{c_r}|\nu_m|A_m \Leftrightarrow \sum_{n=1}^{c_p}|\nu_n|A_n \tag{14}$$

where ν_i is the stoichiometric coefficient, A_i is the reacting species, c_r is the number of reactants, and c_p is the number of products. Recall the convention that the stoichiometric coefficients are negative for the reactants and positive for the products.

Writing a component material balance on the still, we get

$$\frac{dHx_i}{dt}=-Vy_i+\nu_irH \quad (i=1,\ldots,c_r+c_p) \tag{15}$$

and we assume a rate law

$$r=k_f\prod_{m=1}^{c_r}a_m^{|\nu_m|}-k_r\prod_{n=1}^{c_p}a_n^{|\nu_n|} \tag{16}$$

k_f is the forward reaction rate constant, k_r is the reverse reaction rate constant, and the a's are the activities for the components. For liquid-phase reactions, the activities will be represented by the product of the activity coefficient, γ_i, and the mole fraction, x_i: $a_i=\gamma_ix_i$.

Summing Eq. 15 over all the species, we get

$$\frac{dH}{dt}=-V+\nu_TrH \tag{17}$$

where $\nu_T=\sum_{i=1}^{c_r+c_p}\nu_i$. Manipulating Eqs. 15 and 17 in the same manner as Eqs. 2 and 3 and incorporating Eq. 16 give

$$\frac{dx_i}{d\xi}=(x_i-y_i)+\frac{k_fH}{V}(\nu_i-x_i\nu_T)\left(\prod_{m=1}^{c_r}a_m^{|\nu_m|}-\frac{1}{K}\prod_{n=1}^{c_p}a_n^{|\nu_n|}\right)$$
$$[i=1,\ldots,(c_r+c_p-1)] \tag{18}$$

where K is the thermodynamic equilibrium constant defined by

$$K=e^{-(\Delta G^0/RT)} \tag{19}$$

and ΔG^0 is the standard Gibbs energy change of the reaction. At long times the rate equation (Eq. 16) is consistent with thermodynamic equilibrium provided $k_f/k_r=K$. Reaction equilibrium occurs at those temperatures and compositions which satisfy the equation

$$K(T)=\prod_{i=1}^{c_r+c_p}a_i^{\nu_i}=\frac{\prod_{n=1}^{c_p}a_n^{|\nu_n|}}{\prod_{m=1}^{c_r}a_m^{|\nu_m|}} \tag{20}$$

We can rewrite Eq. 18 as

$$\frac{dx_i}{d\xi}=(x_i-y_i)+\frac{H}{H_0}\frac{V_0}{V}\frac{k_f}{k_{f,\min}}Da(\nu_i-x_i\nu_T)$$
$$\times\left(\prod_{m=1}^{c_r}a_m^{|\nu_m|}-\frac{1}{K}\prod_{n=1}^{c_p}a_n^{|\nu_n|}\right)$$
$$[i=1,\ldots,(c_r+c_p-1)] \tag{21}$$

where $Da=(k_{f,\min}H_0)/V_0$ is the Damköhler number. For the general case, we cannot solve Eq. 17 to obtain an explicit relationship between H and H_0 as in the earlier example. We can, however, examine the case where the vapor rate varies in the same way as the holdup, $H/H_0=V/V_0$, which leads to

$$\frac{dx_i}{d\xi}=(x_i-y_i)+\frac{k_f}{k_{f,\min}}Da(\nu_i-x_i\nu_T)\left(\prod_{m=1}^{c_r}a_m^{|\nu_m|}-\frac{1}{K}\prod_{n=1}^{c_p}a_n^{|\nu_n|}\right)$$
$$[i=1,\ldots,(c_r+c_p-1)] \tag{22}$$

This equation reduces to the autonomous model for the simple example discussed in the previous section if we substitute appropriate values for the parameters. We can now apply the more general model to a more complex example, closer to industrial practice, which is the production of methyl tert-butyl ether (MTBE) from isobutene and methanol.

The MTBE example

Methyl tert-butyl ether is an octane blending agent which was the fastest growing chemical in the 1980s. It is made by reacting isobutene and methanol in the liquid phase with temperatures in the range 40 to 100°C using an ion exchange resin (Rehfinger et al., 1990) or sulfuric acid as catalyst (Al-Jarallah et al., 1988b). We consider the case of a sulfuric acid catalyzed reaction. The principal reaction is

$$\text{isobutene} + \text{methanol} \Leftrightarrow \text{MTBE} \qquad (23)$$

Comparing with Eq. 14, the stoichiometric coefficients are $\nu_{m=1} = -1$, $\nu_{m=2} = -1$, $\nu_{n=1} = 1$ and $\nu_T = -1$, and Eq. 22 reduces to two independent equations

$$\frac{dx_i}{d\xi} = (x_i - y_i) + \frac{Da}{k_{f,\min}} r(\nu_i + x_i) \quad (i = 1,2) \qquad (24)$$

where the numbers 1 and 2 stand for the components isobutene, and methanol, respectively.

We obtained a kinetic model as follows. First, we took data from the literature for the thermodynamic equilibrium constant, K, as a function of temperature for the MTBE reaction (Al-Jarallah et al., 1988a). This is shown in Figure 9 as the logarithm of K vs. reciprocal temperature. A linear least-squares fit of the data gives the following temperature dependence for the thermodynamic equilibrium constant

$$\ln(K) = \frac{6{,}820.0}{T} - 16.33 \qquad (25)$$

where the temperature T is in Kelvin. Equation 25 is based on an integrated form of the van't Hoff equation

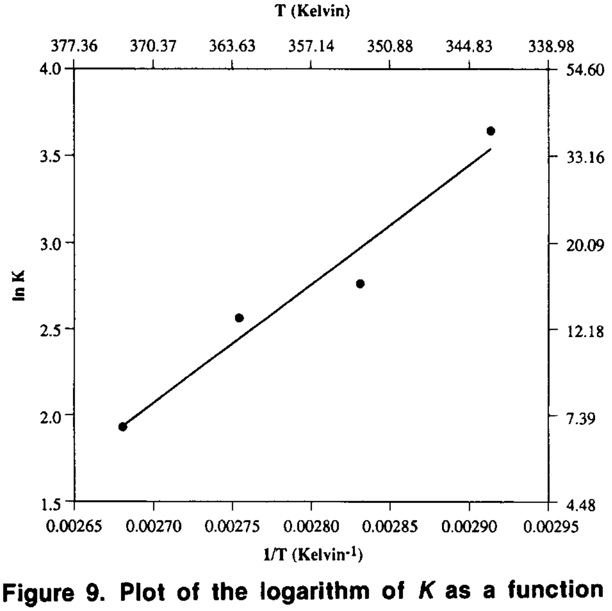

Figure 9. Plot of the logarithm of *K* as a function of reciprocal temperature.

The points are experimental data taken from Al-Jarallah et al. (1988a).

$$\ln(K) = \frac{\Delta H^0}{R}\left(\frac{1}{T} - \frac{1}{T_0}\right) \qquad (26)$$

where ΔH^0 is the heat of reaction (assumed constant over the temperature range of the data), T_0 is a reference temperature, and R is the universal gas constant.

Next, we took molar concentration vs. time data from the literature at different temperatures (at a catalyst concentration of 1% by weight of sulfuric acid) for the MTBE reaction (Eq. 23) carried out in a liquid-phase batch reactor (Al-Jarallah et al., 1988b, 1993). These data were converted to mole fractions using the relation

$$x_i = \frac{\rho_i}{\sum_i \rho_i} \qquad (27)$$

where x_i's are the mole fractions and ρ_i's are the molar concentrations.

For a closed batch reactor (the vapor rate is zero), Eqs. 15 and 17 give

$$\frac{dx_i}{dt} = r(\nu_i - \nu_T x_i) \quad (i = 1, \ldots, c_p + c_r) \qquad (28)$$

where

$$r = k_f\left(\prod_{m=1}^{c_r} a_m^{|\nu_m|} - \frac{1}{K}\prod_{n=1}^{c_p} a_n^{|\nu_n|}\right) \qquad (29)$$

Substituting the values of ν_i and ν_T for the MTBE reaction into Eq. 28 and incorporating the facts that for liquid-phase reactions the activity can be expressed as the product of the liquid mole fraction and the activity coefficient and that the sum of the mole fractions is unity yield the following equations

$$\frac{dx_1}{dt} = r(-1 + x_1)$$
$$\frac{dx_2}{dt} = r(-1 + x_2) \qquad (30)$$
$$\frac{dx_3}{dt} = r(1 + x_3)$$

where

$$r = k_f\left(x_1\gamma_1 x_2\gamma_2 - \frac{1}{K} x_3\gamma_3\right) \qquad (31)$$

The activity coefficients γ_1, γ_2, and γ_3 are well represented by the Wilson equation using parameters reported in Table 2. We solve this model by integrating any two of the differential equations together with the constraint $\sum_1 x_i = 1$.

We fit the mole fraction vs. time data to our kinetic model (Eqs. 30 and 31, with K described by Eq. 25) to obtain the value of the forward reaction rate constant k_f at different temperatures. A plot of the logarithm of the reaction rate

Table 2. Thermodynamic Data for the MTBE Example

Constants for the Antoine Equation

Component	A	B	C	V_i (m^3/mol)
isobutene (1)	20.64556	-2125.74886	-33.160	93.33×10^{-6}
methanol (2)	23.49989	-3643.31362	-33.434	44.44×10^{-6}
MTBE (3)	20.71616	-2571.58460	-34.420	118.8×10^{-6}

Binary Interaction Parameters for the Wilson Equation

$A_{11}=0.0$	$A_{21}=2{,}576.8532$	$A_{31}=271.5669$
$A_{12}=169.9953$	$A_{22}=0.0$	$A_{32}=-406.3902$
$A_{13}=-30.2477$	$A_{23}=1{,}483.2478$	$A_{33}=0.0$

Form of the Antoine Equation

$$\ln(P^{sat}) = A + \frac{B}{T+C}$$

P^{sat} [Pa], T [K]

Wilson Equation

$$\ln(\gamma_i) = 1 - \ln\left(\sum_{j=1}^{C} x_j\Lambda_{i,j}\right) - \sum_{k=1}^{C}\left(\frac{x_k\Lambda_{k,i}}{\sum_{j=1}^{C} x_j\Lambda_{k,j}}\right)$$

where

$$\Lambda_{i,j} = \frac{V_j}{V_i}\exp\left(\frac{-A_{i,j}}{RT}\right) \qquad V_j\ [\mathrm{m^3/mol}], \quad A_{i,j}\ [\mathrm{cal/mol}]$$

constant k_f vs. the reciprocal temperature (see Figure 10) is nearly linear and gives the following Arrhenius expression

$$k_f = 74.40e^{-3{,}187.0/T} \tag{32}$$

where the temperature T is in Kelvin and k_f has the units of inverse minutes.

Figure 11 compares the experimental and calculated values of the mole fraction of methanol as a function of time at a temperature of 353.15 K. The dashed line shows the equilibrium value as predicted by the model. Note that the kinetic model has only *one* adjustable parameter, k_f.

Incorporating the kinetic model into Eq. 24 gives the complete model for the simple distillation of a reactive mixture of isobutene, methanol and MTBE.

$$\begin{aligned}
\frac{dx_1}{dt} &= x_1 - y_1 + \frac{k_f}{k_{f,\min}}\,Da(-1+x_1)\left(x_1\gamma_1x_2\gamma_2 - \frac{1}{K}\,x_3\gamma_3\right)\\
\frac{dx_2}{dt} &= x_2 - y_2 + \frac{k_f}{k_{f,\min}}\,Da(-1+x_2)\left(x_1\gamma_1x_2\gamma_2 - \frac{1}{K}\,x_3\gamma_3\right) \qquad (33)\\
\frac{dx_3}{dt} &= x_3 - y_3 + \frac{k_f}{k_{f,\min}}\,Da(1+x_3)\left(x_1\gamma_1x_2\gamma_2 - \frac{1}{K}\,x_3\gamma_3\right)
\end{aligned}$$

The phase equilibrium is represented by the relation

$$Py_i = P_i^{sat}x_i\gamma_i \tag{34}$$

The Wilson model used to represent the activity coefficients in the rate expression is also used for the VLE calculations. The Antoine equation is used for computing the vapor pressures of the components (see Table 2 for the form of the equations and the values of the constants used in the calculations). We solve this model by integrating any two of the differential equations together with the constraint $\sum_i x_i = 1$.

For calculation, we must specify the operating pressure and the starting liquid composition in the still. In this example, the operating pressure was set at 8 atm. At this pressure, the lowest boiling point is the azeotrope between isobutene and methanol with a composition of 6.7 mol % methanol and a boiling point of 60.2°C. The value of $k_{f,\min}$ at this temperature is 0.0052 min^{-1}. Once the pressure and liquid composition have been

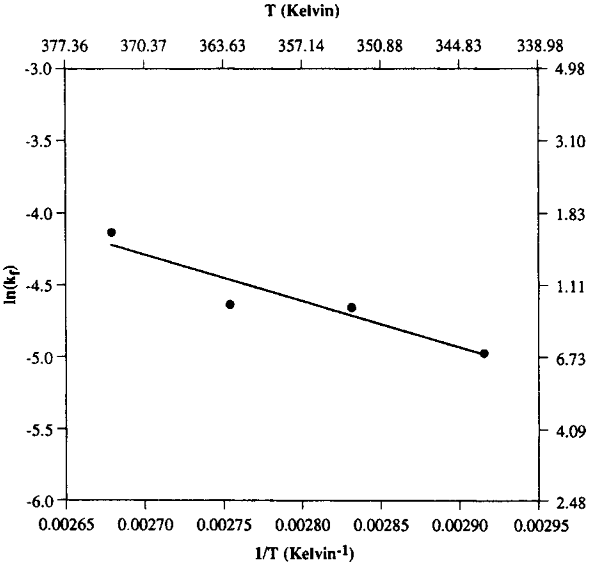

Figure 10. Plot of the logarithm of k_f as a function of reciprocal temperature.

The points represent our fit of values for k_f to the concentration vs. time data of Al-Jarallah et al. (1988b,1993).

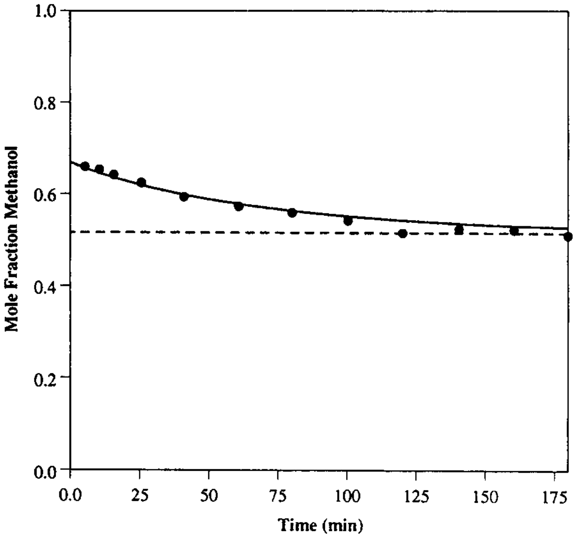

Figure 11. Calculated vs. experimental values of the mole fraction of methanol as a function of time at a temperature of 353.15 K.

The points are experimental data of Al-Jarallah et al. (1988b,1993). The predictions of the kinetic model (—) approach the equilibrium value (- - -) at larger times.

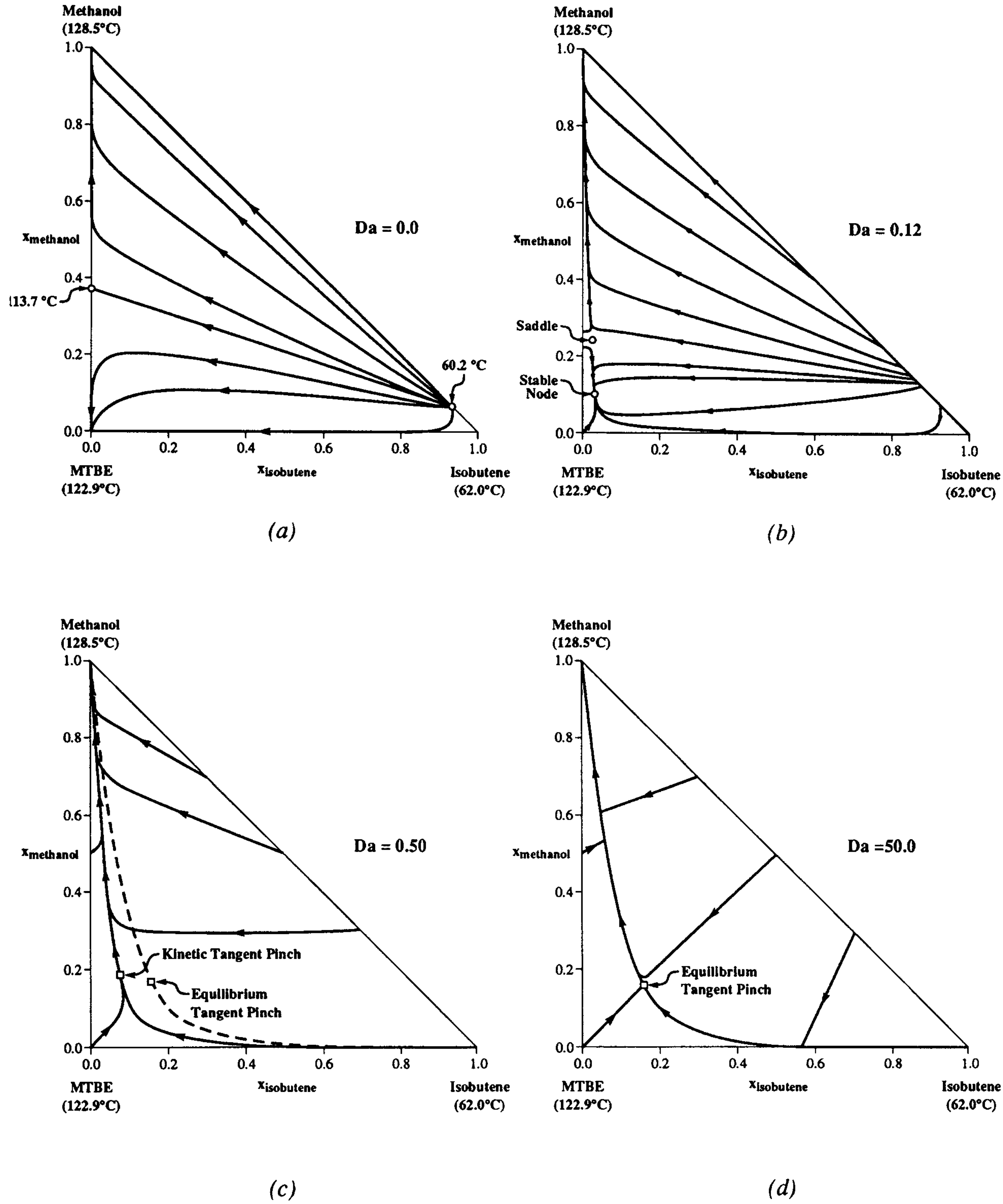

Figure 12. Simple distillation residue curve maps for the MTBE reaction at various values of *Da* and a pressure of 8 atm.

specified, we can determine the vapor composition and the temperature in the system by performing a bubble point calculation. This temperature is then used to evaluate the forward rate constant and the equilibrium constant. This allows us to take one step in the integration of the differential equations. The new liquid composition enables us to obtain a new vapor composition and a new temperature, and so the integration proceeds.

Integrations were performed for a number of initial compositions and many values of the Damköhler number *Da*. Representative results of these calculations are plotted in the phase plane in Figures 12a to 12d.

Results

Figure 12a shows that there are two azeotropes and a distillation boundary in a nonreacting mixture ($Da=0$) of isobutene, methanol and MTBE. The trajectories approach either the pure methanol or the pure MTBE vertex depending on the initial conditions. As we increase the Damköhler number, the stable node at the pure MTBE vertex and the saddle on the methanol-MTBE edge move into the composition triangle (Figure 12b). A bifurcation occurs at a critical Damköhler number of $Da \cong 0.143$, where the stable node and the saddle meet and annihilate each other leaving a tangent pinch behind. For higher values of Da, the only stable node left in the system is the pure methanol vertex and all the trajectories go smoothly to this vertex (Figures 12c and 12d). The behavior of the singular points is summarized in Figure 13. Above $Da \cong 0.143$, the kinetic map is qualitatively similar to the equilibrium reactive map; below $Da \cong 0.143$, the kinetic map is qualitatively similar to the nonreactive map.

Above $Da \cong 0.143$, there is a severe tangent pinch (a very slow change of composition in simple distillation) at these pressures. This is not visible on the residue curve maps although it is an important feature for the production of MTBE in a continuous reactive distillation column (Doherty and Buzad, 1992; Ung and Doherty, 1994a,b,c). As the Damköhler number increases, the tangent pinch moves toward the equilibrium curve, which it finally reaches at large Damköhler numbers (Figure 13).

Since the MTBE reaction is exothermic, an increase in temperature leads to a decrease in the equilibrium constant (Eq. 26), and so the equilibrium curve at lower pressures is closer to the pure MTBE vertex than that at higher pressures. This implies that operating a continuous distillation at lower pressures may yield a product that is richer in MTBE than one operating at higher pressures. This, however, needs to be traded off against the fact that some of the components (such as isobutene) are highly volatile at lower pressures and require refrigeration to condense them.

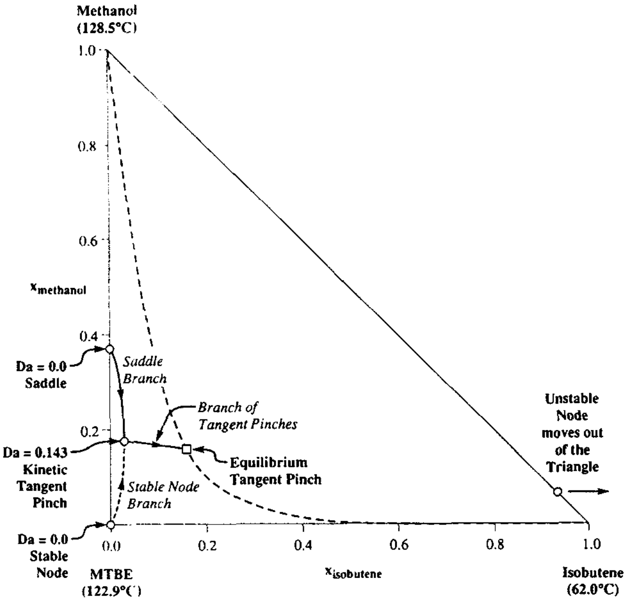

Figure 13. Plot showing the movement of the saddle and stable node for the MTBE reaction as a function of the Damköhler number.

Conclusions

We have derived a model (Eq. 21) that incorporates the effect of chemical kinetics on residue curve maps for reactive distillation. The model agrees with known results for the special cases of equilibrium chemical reaction (Barbosa and Doherty, 1988), and finite-rate reaction with a particular heating policy (Solokhin et al., 1990a,b). It is shown that the heating policy has an effect on the qualitative structure of the model and its solution curves. Rapid heating produces a nonautonomous model with residue curves that intersect in the composition space. Slower heating, however, gives rise to an autonomous model with nonintersecting residue curves.

Residue curve maps generated by the autonomous model can be described by a single parameter, the Damköhler number, which measures the rate of reaction relative to product removal. For small values of the Damköhler number, the nonreactive simple distillation residue curve map is recovered, and the singular points are the pure components and azeotropes in the nonreactive mixture. A bifurcation analysis shows the deformation and, in some cases, the disappearance of these singular points as the Damköhler number is increased until the equilibrium reactive residue curve map is recovered at large values. If the final bifurcation has occurred, the kinetic maps corresponding to intermediate values of the Damköhler number are qualitatively similar to the equilibrium reactive map; for example, a stable node in the kinetic map will lead to a maximum-boiling reactive azeotrope in the equilibrium reactive map. Conversely, if the Damköhler number is below the value corresponding to the final bifurcation, the kinetic map will differ qualitatively from the equilibrium reactive distillation residue curve map, and this bifurcation analysis reveals the limitations of the equilibrium analysis. The ability to manipulate these features will allow greater flexibility in the design of continuous reactive distillation columns.

Acknowledgments

We are grateful for financial support provided by the University of Massachusetts Center for Process Design and Control. We are also grateful to Prof. Adnan Al-Jarallah of the King Fahd University of Petroleum and Minerals, Saudi Arabia, for providing us with additional experimental data, Dr. Sophie Ung of the Department of Chemical Engineering, University of Massachusetts for the thermodynamic data and equilibrium diagram for the MTBE system and Ms. Pam Stephan for drawing the figures. We are also grateful to one of the reviewers for helpful comments.

Notation

a_i = activity of component i
A, A_i, B, C = generic chemical species
c_p = number of products
c_r = number of reactants
Da = Damköhler number ($H_0 k_{f0}/V_0$ dimensionless)
$\underline{f}$ = vector function
ΔG^0 = standard Gibbs free energy change for the reaction
H = liquid molar holdup, mol
H_0 = initial liquid molar holdup, mol
ΔH^0 = standard enthalpy change (heat) of reaction, cal/mol
K = thermodynamic equilibrium constant
k_f = forward reaction rate constant, 1/time

$k_{f,\min}$ = forward rate of reaction at the lowest temperature on the boiling surface, 1/time
k_r = reverse reaction rate constant, 1/time
P = total pressure
P_i^{sat} = saturated vapor pressure for component i
r = rate of reaction
R = universal gas constant
t = time
T = temperature, K
T_0 = reference temperature, K
V = vapor molar flow rate, mol/time
V_0 = initial vapor molar flow rate, mol/time
x_i = mole fraction of component i in the liquid phase
y_i = mole fraction of component i in the vapor phase
$\underline{x}$ = state vector

Greek letters

γ_i = liquid activity coefficient
ϵ = parameter that determines the vapor rate policy
ν_i = stoichiometric coefficient of component i
ν_T = algebraic sum of the stoichiometric coefficients of the components in the reaction
θ = time variable defined after Eq. 35
ρ_i = molar concentration of species i
ξ = "warped" time variable defined after Eq. 5, $\xi = \ln(H_0/H)$

Subscripts

A, B, C = components A, B, and C
i = component i
m = reactants
n = products
0 = initial value
1, 2, 3 = components A, B, and C

Literature Cited

Agreda, V. H., and L. R. Partin, "Reactive Distillation Process for the Production of Methyl Acetate," U.S. Patent No. 4,435,595 (Mar. 6, 1984).

Agreda, V. H., L. R. Partin, and W. H. Heise, "High-Purity Methyl Acetate via Reactive Distillation," *Chem. Eng. Prog.*, **86**(2), 40 (1990).

Al-Jarallah, A. M., M. A. B. Siddiqui, and A. K. K. Lee, "Kinetics of Methyl Tertiary Butyl Ether Synthesis Catalyzed by Ion Exchange Resin," *Can. J. of Chem. Eng.*, **66**, 802 (1988a).

Al-Jarallah, A. M., A. K. K. Lee, and M. A. B. Siddiqui, "Kinetics of Methyl Tertiary Butyl Ether Synthesis Catalyzed by Sulfuric Acid," *Chem. Eng. J.*, **39**, 169 (1988b).

Al-Jarallah, A. M., private communication (1993).

Barbosa, D. A. G., and M. F. Doherty, "The Simple Distillation of Homogeneous Reactive Mixtures," *Chem. Eng. Sci.*, **43**, 541 (1988).

Davies, T. V., and E. M. James, *Nonlinear Differential Equations*, Addison-Wesley, Reading, MA (1966).

Doherty, M. F., and G. Buzad, "Reactive Distillation by Design," *Trans. I. Chem. Eng.*, **70**, 448 (1992).

Grosser, J. H., M. F. Doherty, and M. F. Malone, "Modeling of Reactive Distillation Systems," *Ind. Eng. Chem. Res.*, **26**, 983 (1987).

Rehfinger, A., and Ulrich Hoffmann, "Kinetics of Methyl Tertiary Butyl Ether Liquid Phase Synthesis Catalyzed by Ion Exchange Resin: I. Intrinsic Rate Expression in Liquid Phase Activities," *Chem. Eng. Sci.*, **45**, 1605 (1990).

Sansone, G., and R. Conti, *Nonlinear Differential Equations*, Pergamon Press, New York (1964).

Smith, L. A., "Catalytic Distillation Process," U.S. Patent No. 4,307,254 (Dec. 22, 1981).

Smith, L. A., "Method for the Preparation of Methyl Tertiary Butyl Ether," U.S. Patent No. 4,978,807 (Dec. 18, 1990).

Solokhin, A. V., S. A. Blagov, L. A. Serafimov, and V. S. Timofeev, "Open Evaporation Processes Accompanied by Chemical Reaction in the Liquid Phase," *Theor. Found. Chem. Eng.*, **24**(2), 103 (1990a).

Solokhin, A. V., S. A. Blagov, L. A. Serafimov, and V. S. Timofeev, "Dynamical System for Open Evaporation Process in Presence of A⇔B Chemical Reaction," *Theor. Found. Chem. Eng.*, **24**(5), 377 (1990b).

Ung, S., and M. F. Doherty, "Vapor-liquid Phase Equilibrium in Systems with Multiple Chemical Reactions," *Chem. Eng. Sci.*, in press (1994a).

Ung, S., and M. F. Doherty, "Calculation of Residue Curve Maps for Mixtures with Multiple Equilibrium Chemical Reactions," *Ind. Eng. Chem. Res.*, in press (1994b).

Ung, S., and M. F. Doherty, "Synthesis of Reactive Distillation Systems with Multiple Equilibrium Chemical Reactions," *Ind. Eng. Chem. Res.*, in press (1994c).

Appendix: Asymptotic Analysis for the Autonomous Model

Equation 9 can be rewritten as

$$\frac{dx_i}{d\theta} = \frac{x_i - y_i}{Da} - \left(x_1 x_2 - \frac{x_3^2}{K}\right) \quad (i = 1,2) \tag{A1}$$

where

$$d\theta = (Da)\,d\xi \tag{A2}$$

For large values of Da and initial conditions far from equilibrium, the first term on the righthand side of Eq. A1 is very small when compared to the second term. Therefore, neglecting the first term, Eq. A1 may be written as

$$\frac{dx_i}{d\theta} \approx -\left(x_1 x_2 - \frac{x_3^2}{K}\right) \quad (i = 1,2) \tag{A3}$$

Writing out the equations individually and dividing the second by the first, we get

$$\frac{dx_2}{dx_1} = 1 \tag{A4}$$

Equation A4 implies that for initial conditions far from equilibrium, for systems with large Damköhler numbers, the initial slope of the residue curves should be unity. Figures 4 and 5 satisfy this condition.

It may be noted that these results agree with the equilibrium theory. The lines with a slope of unity are identical to the stoichiometric lines of constant transformed composition described by Barbosa and Doherty (1988). In the equilibrium theory, trajectories approach the reaction equilibrium curve with infinite speed and, on reaching it, move along the equilibrium curve at a finite speed.

Manuscript received Mar. 3, 1994, and revision received June 9, 1994.